



Investigation of mechanical properties and fracture surfaces of dual-phase 60–40 brass alloy processed by warm equal-channel angular pressing

Seyed Elias Mousavi^{1,*}, Mahmood Meratian¹, and Ahmad Rezaeian¹

¹Department of Materials Engineering, Isfahan University of Technology, Isfahan 8415683111, Iran

Received: 2 January 2017

Accepted: 13 March 2017

Published online:
24 March 2017

© Springer Science+Business
Media New York 2017

ABSTRACT

In this study, the effect of equal-channel angular pressing process on the mechanical properties of a dual-phase 60–40 brass alloy was investigated. The samples were processed up to six passes through the route C at 350 °C. Optical microscopy and tensile tests were employed for the investigation of microstructure and mechanical properties. Increasing the number of passes caused the increase in both strength and elongation. It was observed that by the sixth pass, the elongation at the room temperature was increased up to 85% and the tensile strength was obtained to be 1.5 times more than that of the annealed sample. Micro-hardness test results also showed that the hardness was increased to 100% for the specimen processed to the sixth pass. Since the process temperature was less than $T_m/2$, due to the low stacking-fault energy of this alloy, continuous recrystallization was expected to occur in the microstructure. However, it was observed that recrystallized grains were formed near the grain boundaries for the first pass. To determine the type of the recrystallization, primary specimens were rolled up to 95% and then annealed at different temperatures. The obtained samples microstructures confirmed that both static and dynamic recrystallizations occurring in the primary passes were the reason for the bimodal structure formation in these passes. To study the fracture surfaces, scanning electron microscope was employed. The results showed the ductile fracture in all the specimens. By increasing the passes, this type of fracture was expanded.

Introduction

Nowadays, three decades after the invention of severe plastic deformation processes, their effective role in the grain refinement has been well substantiated.

Some of the most important severe plastic deformation processes are equal-channel angular pressing (ECAP), high-pressure torsion (HPT) and accumulative roll bonding (ARB). Among them, the ECAP process has been found to be the most efficient by

Address correspondence to E-mail: se.m201a@gmail.com; Elias.Mousavi@ma.iut.ac.ir

many industrial and academic researchers as it is the only process producing high-strength rod-shaped specimens. Through the ECAP process, the specimens are passed through two crossed channels with the same cross section; by following each pass, some severe shear stress is applied to them [1–9]. Since the cross section of inlet and outlet channels is equal, dimensional divergences do not occur in the specimen; this considered as the main distinguishing feature of this process, as compared with other deformation processes. This phenomenon causes the stored energy and dislocation density to increase dramatically, leading to grain refinement [10, 11]. Compared to the other strengthening methods such as solid solution, precipitation hardening and second phase, which reduce elongation, such a process simultaneously causes both strength and elongation [12]. The effect of this process on the mechanical properties of the dual-phase brass alloy has not been investigated much due to its low stacking-fault energy. The low stacking-fault energy eliminates the possibility of the process at room temperature. As a result, to apply more strain to reach fine grain sizes, the process may be conducted at elevated temperatures. It is obvious that elevating the sample temperature can cause the grain growth, which is the main weakness of the process in such alloys. Dutkiewicz et al. [13] studied the effect of the process on the dual-phase brass containing 1.5% lead in limited passes and different routes. Nishi et al. [14] reported the superplastic behavior of this alloy after the single pass. Also, in a similar study, they reported the effect of the process on the super plasticity of the dual-phase brass containing tin [15]. Kim et al. [16] investigated alterations in the mechanical properties of the 60–40 brass alloy processed by ECAP conducted at 250 °C in the route A. The weakness of their study was dramatic reduction in elongation by increasing the number of passes, which could be attributed to the non-occurrence of recrystallization in the process. In this study, the mechanical properties of specimens were studied after different passes of the process using the die with 120° that 65% strain applied in each pass [17]. Also, it was tried to explain the behavior of the alloy at room temperature through relating tensile test and micro-hardness test results. In addition, since the recrystallized grains observed in the primary passes of the process were not anticipated, by using rolling–annealing treatment, the types of recrystallization were investigated.

Finally, fracture surfaces of the specimens were studied to reveal the type of the fracture.

Experimental procedures

The as-cast 60–40 brass alloy was first homogenized and then forged at 750 °C to eliminate the casting defects. A typical chemical composition of the as-received samples is shown in Table 1. Then, to increase formability and reach an equiaxial grain structure, the specimens were annealed at 400 °C for 2 h. The specimens were 20 mm in diameter and 50 mm in length. The ECAP process was conducted in a die with 120° internal angle and 20° curvature angle at 350 °C for six passes in the route C, such that each specimen was turned 180° after each pass. Also, the MoS₂ was sprayed to the die as the lubricating material to reduce the friction. For microstructural studies, specimens were cut in the pressing direction. Metallographic specimens were etched in a chloro ferric solution (5% iron chloride, 2 ml hydro chloridric and 95% methanol). Microstructural investigations were conducted using an Olympus optical microscope. To determine the static recrystallization temperature, primary specimens were rolled. The rolling machine induced 1 mm reduction in each rolling pass. Thus, after 27 passes of rolling, the primary thickness was reduced by 95%. To study alpha phase hardness, the microhardness test was conducted with 50gr of load and 15 s of dwell time. The tensile test was conducted through the ASTM standard [18] with specimens of 1.5 mm thickness in the press direction, as cut from processed specimens. This test was conducted using H50KS Hounsfield machine at the steady velocity of 0.5 mm/s and the room temperature. The results of X-ray diffraction tests applied by a Philips X'pert MPD machine were used to study phase transformation during the deformation process. Also, the fracture surfaces of the tensile test specimens were investigated using Philips XL30 scanning electron microscope.

Table 1 Weight percent of brass alloy

Elements	Cu	Zn	Pb	Other elements
Weight percent	60.17	39.82	0.003	Remnant

Experimental results

Microstructures

Figure 1 shows the microstructure of specimens after different passes. As can be seen, recrystallized grains were formed in the structure after the first pass of the process. These fine grains in the third pass were formed in a large portion of the structure, reaching a saturation state in the last two passes. It is noteworthy that through the even passes, one could observe a trend showing the change in the morphologies and reduction in grain sizes and phase elongation. Table 2 shows grain sizes for different numbers of passes. For odd passes with bimodal structures, fine and coarse separate grains were reported. For the second pass, grain migration caused grain growth and mean grain size was increased, as compared to the primary grain size shown in Fig. 1. By increasing the passes, fine grains were developed gradually and

a homogenized structure was formed (Fig. 1). About this phenomenon, Jiang et al. [19] investigated the evaluation of grains orientation and texture by increasing the number of passes in copper. However, it must be noted that pure copper due to its moderate stacking-fault energy has a different deformation behavior as compared to the brass alloy.

Mechanical properties

Since the size of the beta grain was reduced by increasing the number of passes, it was impossible to carry out the micro-hardness test on this phase. Figure 2 shows micro-hardness variations in the base alpha phase against the number of passes in the route C. As can be seen, by increasing the passes, hardness was gradually increased. After the first pass, the hardness was increased to 126 HV, and by following the second pass, it reached 141HV. The graph slope was reduced after two passes; finally, in the sixth

Figure 1 Microstructure of the specimens in the: **a** first, **b** second, **c** third, **d** forth, **e** fifth and **f** sixth pass.

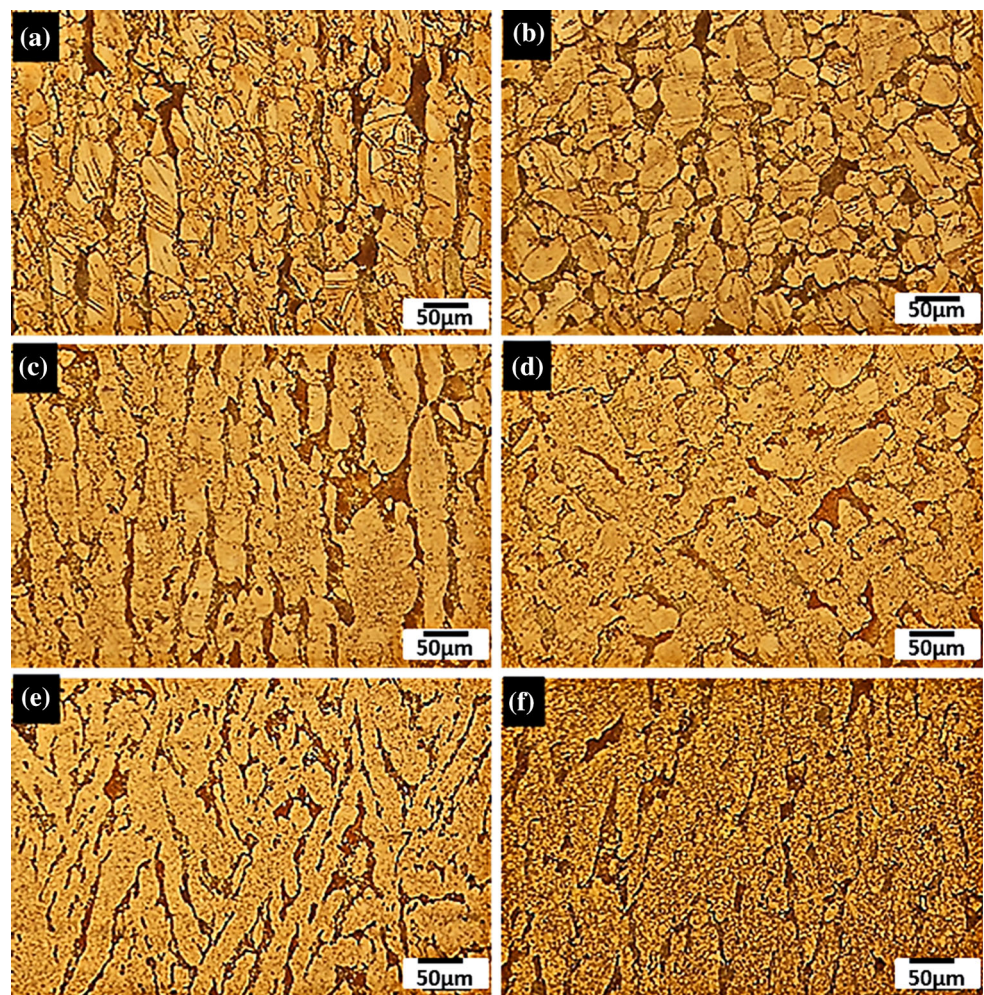
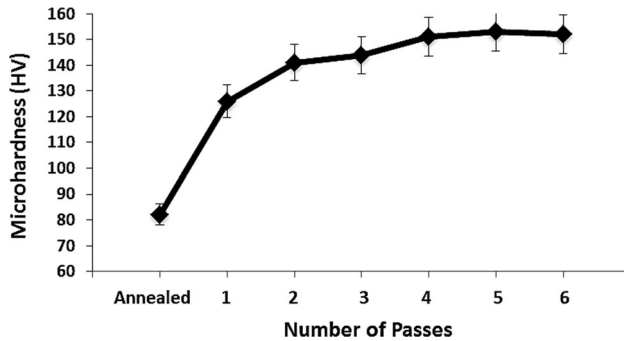
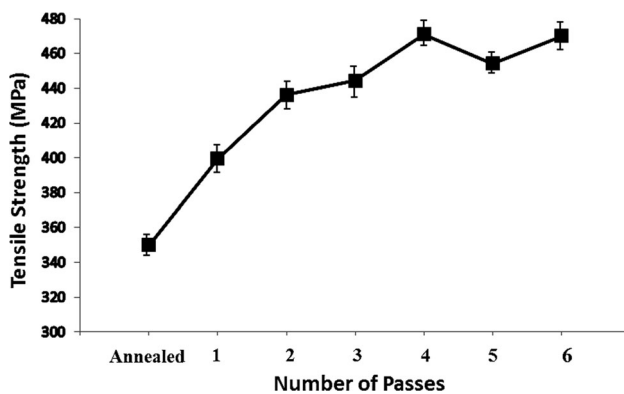


Table 2 Mean grain size in different numbers of passes

Number of passes	1	2	3	4	5	6
Fine grain size (μm)	0.9 ± 0.5	–	2.2 ± 1.1	2.9 ± 1	0.5 ± 0.3	0.7 ± 0.2
Coarse grain sizes	13.3 ± 3.4	23.5 ± 2	21 ± 2.2	22 ± 3	–	–

**Figure 2** Micro-hardness variations with increasing the number of passes in route C.**Figure 3** Tensile strength variation with increasing the number of passes in route C.

pass, it was 1.5 times more than that of the annealed specimen. In the third pass, the slope of the hardness graph was reduced due to the beginning of the recrystallization in the structure (Fig. 1c). By the beginning of recrystallization, the conditions tended to promote the work hardening of new grains; thus, micro-hardness was increased sharply. It was observed that the slope of the graph in the last three passes was close to zero. In other words, in the last three passes, work hardening (creation and pinning of the dislocations) and work softening (recovery and recrystallization) were realized equally, reaching a constant amount.

Figure 3 shows variation in tensile strength versus the number of passes. As can be seen, tensile strength increment showed a trend somewhat similar trend to

the micro-hardness increment in Fig. 2. By the initiation of deformation in the first pass, tensile strength was increased up to the fourth pass and then reached the steady state. Table 3 shows elongation variations versus the number of passes. One could observe that elongation had a different trend; it was reduced with increasing the number of passes then increased up to 85% in the last pass.

Figure 4 shows fracture surfaces of different specimens obtained from the tensile tests. As can be seen, in all specimens, numerous dimples existed, indicating the ductile fracture. In the first pass, dimples were deeper, with significant cleavages indicating the presence of the brittle beta phase. By increasing the passes, the cleavages attributed to the beta phase were reduced in size and the number of dimples was increased. In fact, by increasing the passes, dimples were reduced in size, becoming shallower. This could be attributed to stress distribution of finer grains by increasing passes or the elimination of stress from the primary coarse grains. Furthermore, by increasing the passes, dimple elongation and closure were seen, showing the shear stress applied to them. Also, by increasing the number of passes, a more uniform distribution of dimple sizes was seen, indicating equiaxed grains and a uniform deformation in these passes.

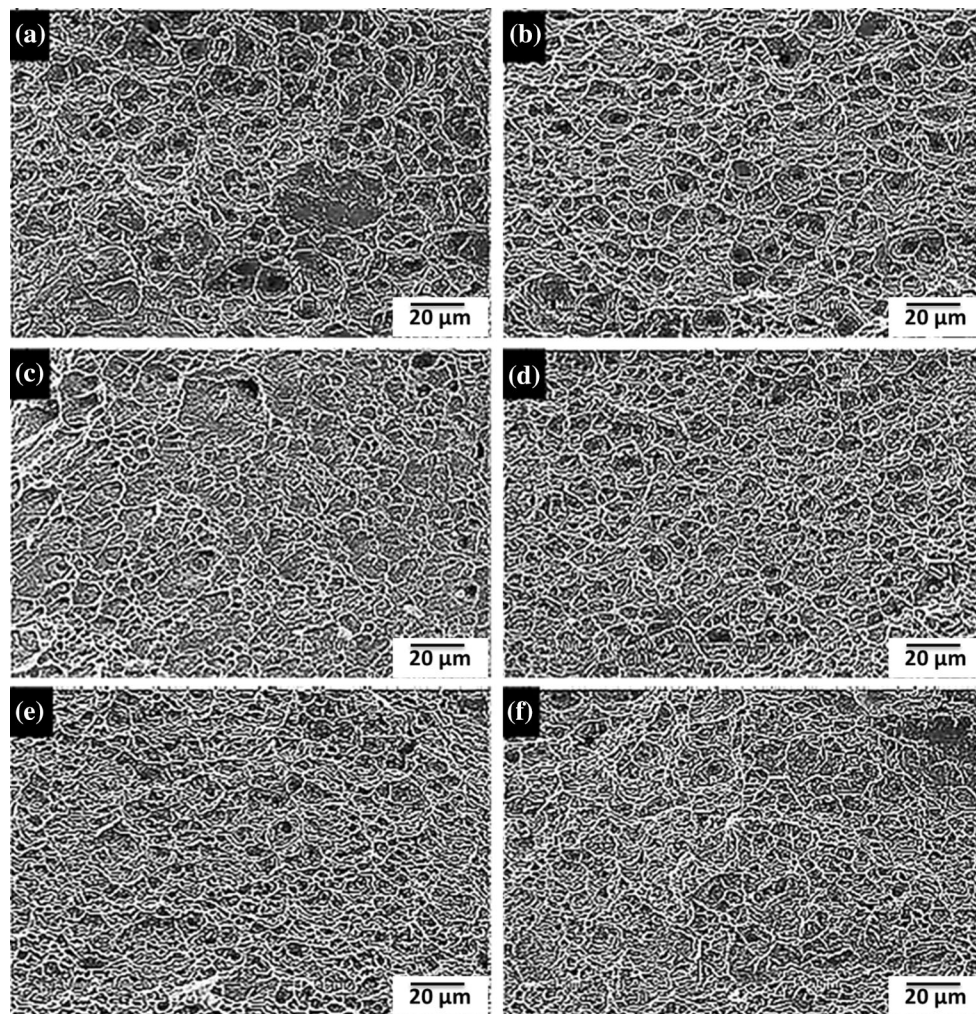
Discussion

Variation in grains morphologies

The variation in morphologies in different grains occurred, as shown in Fig. 1, by increasing the number of passes. One could observe in the first, third and fifth passes that the shear stress applied in the deformation zone of the die caused grain boundary elongation. On the other hand, in the second, fourth and sixth passes, due to the 180° rotation of the specimen, the stress was applied in a reverse direction, causing grains to become equiaxed. Su et al. [20] conducted this investigation on the magnesium alloy, reporting such a behavior. Of course, it

Table 3 Elongation variation with increasing the number of passes in route C

Number of passes	Annealed	1	2	3	4	5	6
Elongation percent	110 ± 9.8	69 ± 6.9	61 ± 4.9	77.2 ± 5.2	76.8 ± 5.3	66.7 ± 4.7	84.9 ± 5.5

**Figure 4** Fracture surface of specimens from the tensile test after the: **a** first pass, **b** second pass, **c** third pass, **d** fourth pass, **e** fifth pass and **f** sixth pass.

must be noted that the magnesium alloys have an HCP crystalline structure enjoying a different deformation behavior, as compared to the alloy investigated in this study. Figure 5 schematically depicts tensile and compressed grains in odd and even passes. The primary grains after the first pass were elongated in the deformation zone of the die. In the second pass of the deformation, specimens were 180° rotated, and thus, slip traces coincided with the previous trace. Variation in stress direction caused

compressed and relatively coaxial grains. This cycle was repeated in other odd and even passes.

As can be seen from Fig. 1, by increasing the number of passes, beta phase width was gradually decreased and transformed to small islands. The width reduction could be attributed to the proximity of the brittle and ductile phases of alpha. Figure 6 gives the schematic representation of the beta phase necking. The ductile alpha phase was yielded and deformed in different passes of the process. By

Figure 5 Schematic of elongation and compression of grains in odd and even phases.

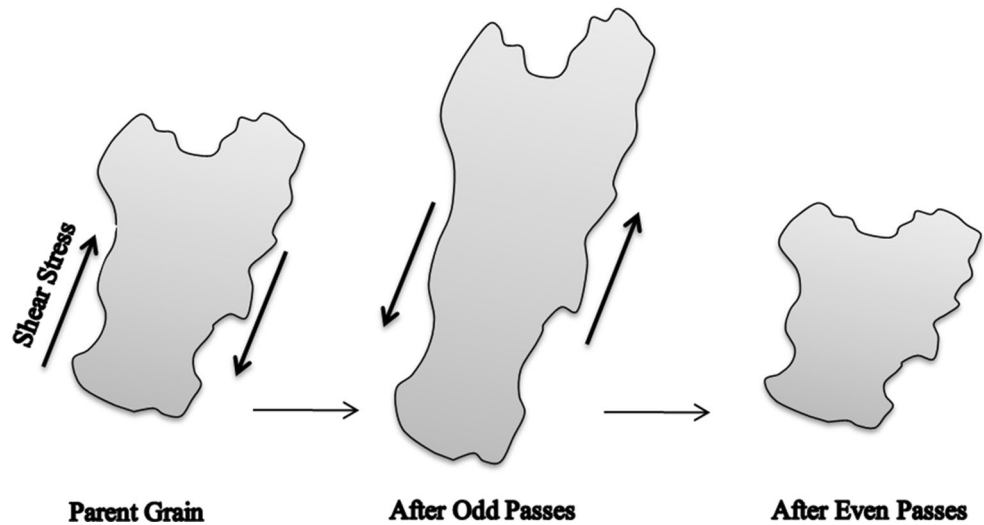
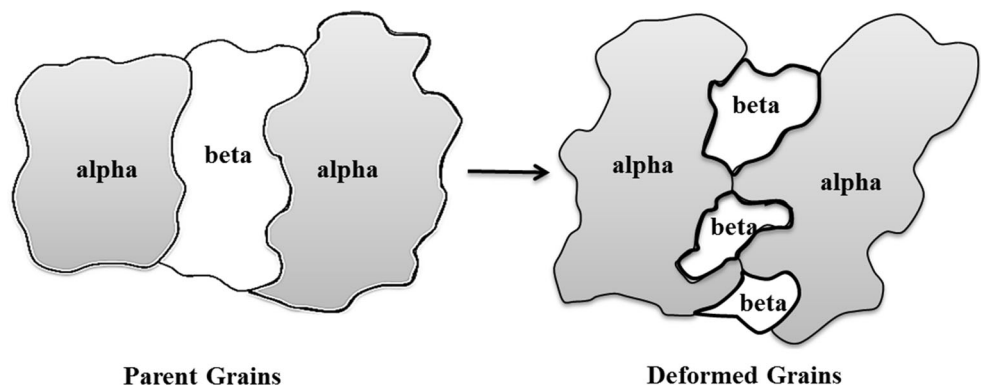


Figure 6 Transformation of beta phase grains to small islands by increasing number of passes.



increasing passes, alpha phase was work-hardened, overcoming the strength of the beta phase. Consequently, by applying higher-amplitude stresses, beta was transformed to small islands. This mechanism could also facilitate recrystallization in the beta phase since these small islands are surrounded by work-hardened alpha grains and more stresses are applied on the beta phase walls.

Determination of recrystallization type using the rolling process

Since the process temperature was lower than $0.5T_m$, according to the literature, continuous dynamic recrystallization was anticipated [21]. However, as can be seen in Fig. 1, despite the expectation, discontinuous dynamic recrystallization was confirmed to occur. Also, sizes of the recrystallized grains were higher than those anticipated for dynamic recrystallized grains. However, it was possible that due to the low stacking-fault energy for this alloy and the

capacity of the alloy to form annealing twins, energy was accumulated in the material, thereby dramatically reducing the dynamic recrystallization start temperature. To resolve this ambiguity, the static and dynamic recrystallization temperatures had to be measured separately. For the static recrystallization temperature measurement, the microstructure and micro-hardness of the alloy were studied after cold work and annealing heat treatment at different temperatures. Cold rolling was conducted to the maximum thickness reduction, and the annealed microstructure was studied.

Figure 7 shows the microstructures of the specimens for 95% cold rolling and after annealing at different temperatures for 10 min. As can be seen, static recrystallization was started at 300–350 °C, while grain growth was started from 450 to 500 °C (Figs. 1, 7). It is worth mentioning that alpha phase grain size at 300 °C was about $3 \pm 1 \mu\text{m}$ (close to the grain size at the first pass in Table 2); by raising the temperature, it was gradually increased. Figure 8

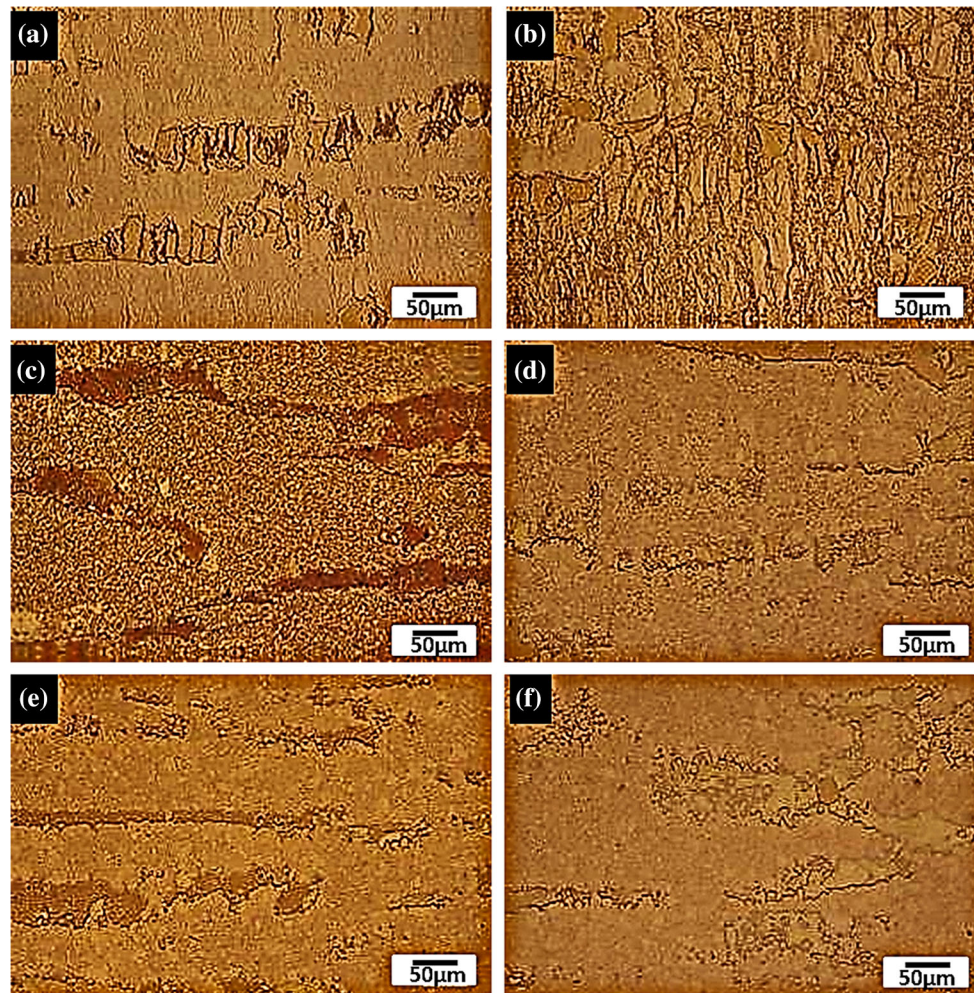


Figure 7 Microstructure of the rolled specimens after 10 min of annealing at temperatures of: **a** 250 °C, **b** 300 °C, **c** 350 °C, **d** 400 °C, **e** 450 °C and **f** 500 °C.

shows hardness variation versus annealing temperature, thereby supporting the results shown in Fig. 7. As can be seen, by increasing the temperature from 300 °C, hardness was reduced, representing the static recrystallization initiation. On the other hand, according to the literature, in the compression test employed for this alloy, dynamic recrystallization starts at 400–650 °C at different strain rates and 30% strain [22, 23]. Since the strain is highly concentrated in the ECAP process, as compared to the compression test, it was anticipated that the dynamic recrystallization would start at temperatures below 400 °C.

Figure 9 shows some dynamically refined grains in the first pass that were formed in the grain, as well as phase boundaries. The size of these grains was less than 1 μm. In static recrystallization, since grain boundaries have more time to migrate, the grains are

normally formed in the larger sizes. On the other hand, as mentioned earlier, grain size for the first pass specimens was close to that of the roll-annealed specimens ($3 \pm 1 \mu\text{m}$). Thus, in the first passes, the static recrystallization had a more critical role than the dynamic recrystallization. Therefore, the occurrence of both static and dynamic recrystallizations in the ECAP process conducted at 350 °C was much likely to happen.

Elongation variation

It was observed that in contrast to what was anticipated, the elongation did not increase continuously. Normally, in the alloys formed by different deformation processes, dislocation densities and grain boundaries are increased. The dislocations are

Figure 8 Micro-hardness variation versus annealing temperature of the rolled specimens.

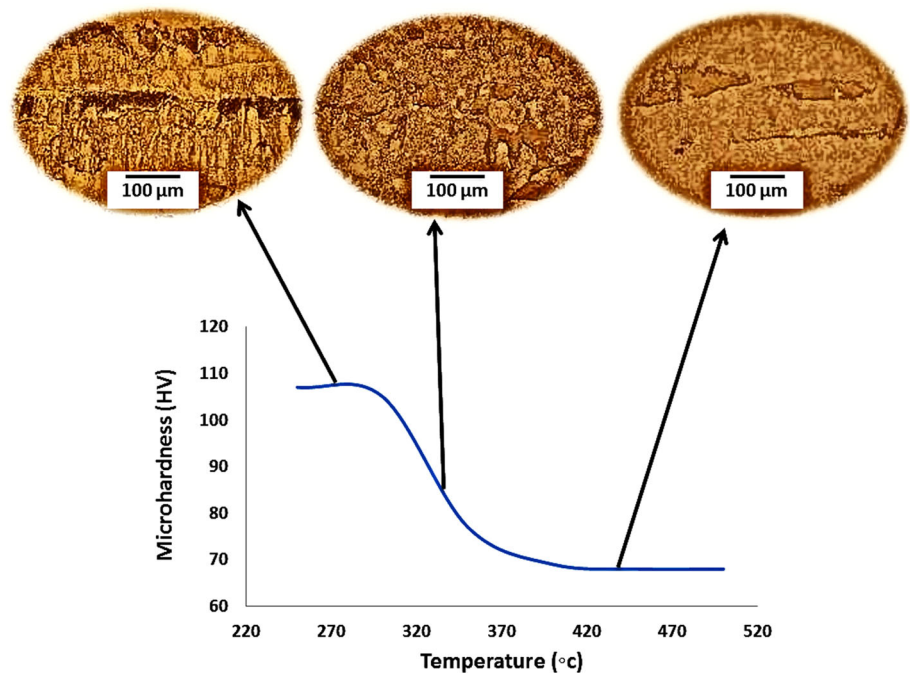
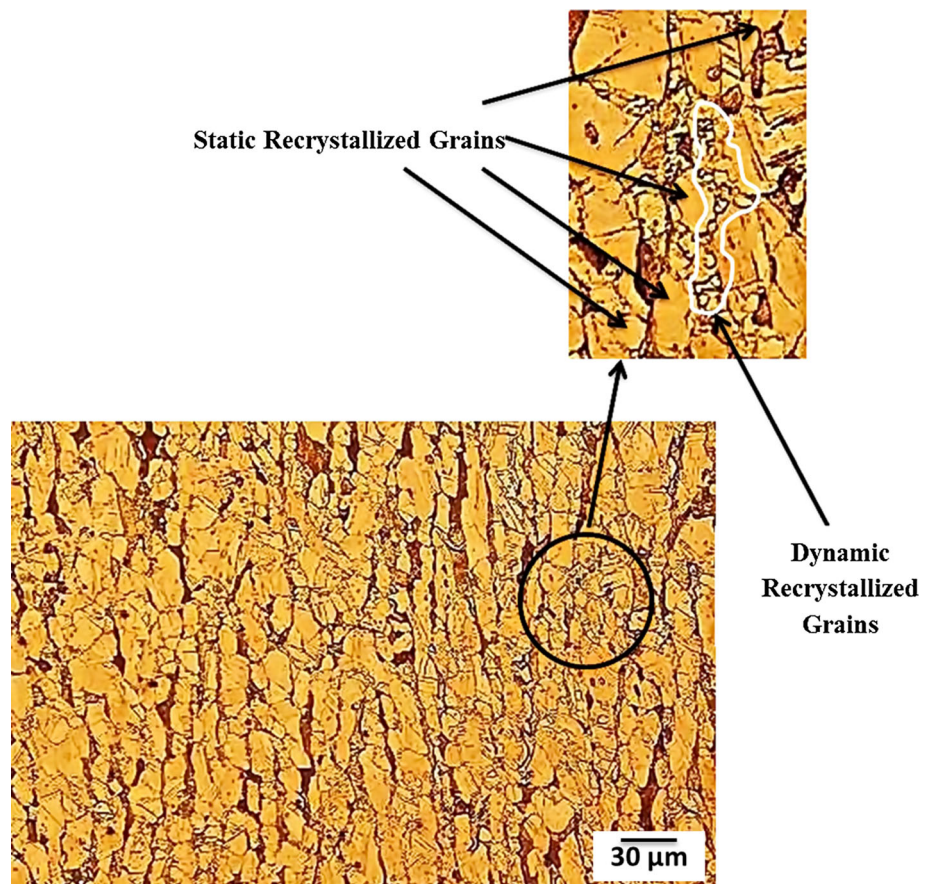


Figure 9 Dynamically recrystallized grains in the first pass of the ECAP process at 350 °C.



accommodated behind these obstacles and pinned. Thus, the strength is increased and the elongation is reduced. However, as shown in Table 3, contrary results were obtained. To explain this, it should be noted that variation in stain traces in different passes, formation of bimodal structures in some passes and development of coaxial recrystallized grains could affect the tensile properties of the alloy competitively. Each of these items could control the tensile behavior of the material in different conditions.

From Table 3, it could be seen that in the first pass, the strength was increased and the elongation was reduced, as compared to the annealed specimen. In the second pass, the strength was increased and the elongation was reduced. In the third pass, despite an increase in the strength, the elongation was not increased, as compared to the second pass.

As shown in Fig. 1, the recrystallization began from the first pass, causing the bimodal structure. Recrystallized fine grains were created in the first pass and grown in the second pass (23 μm). Then, the bimodal structure with more recrystallized grains was formed in the third pass. A mixture of fine and coarse grains caused both elongation and strength to improve. In these circumstances, fine grains prevented the dislocation movement and increased the strength. On the other hand, coarse grains made space for dislocations slip with no grain boundary obstacles, thereby increasing the elongation. Therefore, in passes in which a bimodal structure was formed, both elongation and strength were improved simultaneously. In addition, due to the dynamic recovery that was approximately done on the second pass, dislocations could move easily in the third pass. This could be another reason for not reducing elongation in this pass. According to Fig. 2, in the fourth pass, the micro-hardness value was increased with a sharper slope, as compared to other passes. However, tensile strength was increased, as compared to the previous pass, while the elongation did not change significantly. In this pass, the specimen enjoyed a more homogenized structure including more fine grains (Fig. 1 and Table 2), thereby increasing the strength (Fig. 3). Also, a larger number of recrystallized grains were formed in the structure (Fig. 1). All these showed that most of the recrystallization was conducted due to the accumulated energy in the previous passes after exiting the specimen in the third pass during heating for the fourth pass (before deformation). In such conditions, a larger number of

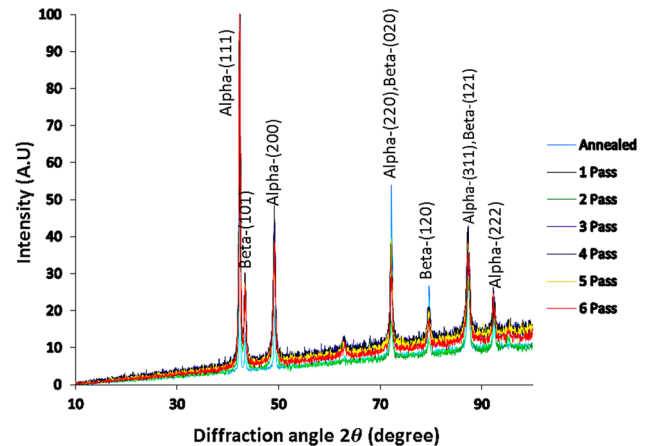


Figure 10 XRD patterns for different passes of ECAP at 350 °C.

recrystallized fine grains could enhance the elongation. Since dislocations could cause a great amount of strain in new grains free of stress, the induced work hardening could also increase the strength in the majority of the grains. In the fifth and sixth passes, the equilibrium structure was formed in the specimen and the formerly recrystallized grains were transformed to the finer ones (0.5–0.7 μm).

Table 3 shows that elongation increment in the sixth pass was about (85%), which could be attributed to phase transformation due to strain. In this condition, the beta phase was transformed to the ductile alpha phase; therefore, alloy deformation could be conducted more easily at lower stresses. To investigate this phase transformation, the specimens were studied using the X-ray diffraction. Figure 10 shows the XRD results. It could be seen that all peaks were nearly the same and coincided each other, showing that no phase transformation had occurred; thus, this could not be a suitable reason for the increased ductility. It is believed that in such conditions, due to sample rotation and recovery, as well as propagation of fine beta phase recrystallized grains (Fig. 1), the elongation could be increased in the last two passes. In other words, up to the fourth pass, the alpha phase was controlling the deformation behavior, while in the last two passes, the propagation of recrystallized grains in the beta phase also helped the ductility of the material.

Conclusions

- Microstructural studies of the specimens in different passes showed that the grains were

elongated in odd passes and equiaxed in the even ones. The reason for this phenomenon was coincidence of slip systems on each other, which occurred by the 180° rotation of specimen.

- By the third pass, the grains were ultra-fined and propagated all over the structure by increasing the number of passes. In the fifth pass, the structure reached a uniform and saturated state, and the size of these recrystallized grains was reduced to 500 nm.
- By increasing passes, the beta phase was fragmented into smaller islands. The reason was the flow of the neighboring α phase and application of the stress controlling its resistance.
- Optical microscope images showed that the occurrence of the discontinuous static recrystallization was possible in the processed specimens. Also, ultra-fine grains were formed in the boundaries and sizes of some of them reached less than 1 μm , indicating dynamic recrystallization.
- Micro-hardness test results showed that in the last two passes of deformation, alloys reached a relatively stable state. In contrast to the primary passes, work softening restrained work hardening induced by the increasing number of passes. Also, optical micrographs of the structure showed the saturation of the fine recrystallized grains.
- Tensile strength variation in the specimens had a trend similar to that of micro-hardness. The studies indicated that in the last pass; elongation was increased, reaching about 85%. XRD patterns also proved that phase transformation was not the cause of elongation in the final pass. So more work softening in the beta phase improved the elongation.
- The study of the fracture surface of the specimens using electron microscope showed that after the first pass, the ductile fracture occurred in the specimens. Also, by increasing the number of passes, the number of dimples was increased and their size was reduced. This indicated propagation of fine grains in the microstructure by increasing the number of passes.

Acknowledgement

This research was supported by Isfahan University of Technology.

Compliance with ethical standards

Conflict of interest The authors declare that they have no conflict of interest.

References

- [1] Gholinia A, Prangnell PB, Markushev MV (2000) The effect of strain path on the development of deformation structures in severely deformed aluminum alloys processed by ECAE. *Acta Mater* 48:1115–1130. doi:[10.1016/S1359-6454\(99\)00388-2](https://doi.org/10.1016/S1359-6454(99)00388-2)
- [2] Segal VM (1995) materials processing by simple shear. *Mater Sci Eng A* 197:157–164. doi:[10.1016/0921-5093\(95\)09705-8](https://doi.org/10.1016/0921-5093(95)09705-8)
- [3] Iwahashi Y, Horita Z, Nemoto M, Langdon TG (1998) The process of grain refinement in equal-channel angular pressing. *Acta Mater* 46:3317–3331. doi:[10.1016/S1359-6454\(97\)00494-1](https://doi.org/10.1016/S1359-6454(97)00494-1)
- [4] Valiev RZ, Islamgaliev RK, Alexandrov IV (2000) Bulk nanostructured materials from severe plastic deformation. *Prog Mater Sci* 45:103–189. doi:[10.1016/S0079-6425\(99\)00007-9](https://doi.org/10.1016/S0079-6425(99)00007-9)
- [5] Segal VM (1999) Equal channel angular extrusion: from macromechanics to structure formation. *Mater Sci Eng A* 271:322–333. doi:[10.1016/S0921-5093\(99\)00248-8](https://doi.org/10.1016/S0921-5093(99)00248-8)
- [6] Zhu YT, Lowe TC (2000) Observations and issues on mechanisms of grain refinement during ECAP process. *Mater Sci Eng A* 291:46–53. doi:[10.1016/S0921-5093\(00\)00978-3](https://doi.org/10.1016/S0921-5093(00)00978-3)
- [7] Iwahashi Y, Horita Z, Nemoto M, Langdon TG (1997) An investigation of microstructural evolution during equal-channel angular pressing. *Acta Mater* 45:4733–4741. doi:[10.1016/S1359-6454\(97\)00100-6](https://doi.org/10.1016/S1359-6454(97)00100-6)
- [8] Furukawa M, Horita Z, Nemoto M, Langdon TG (2001) Review: processing of metals by equal-channel angular pressing. *J Mater Sci* 36:2835–2843. doi:[10.1023/A:1017932417043](https://doi.org/10.1023/A:1017932417043)
- [9] Valiev RZ, Langdon TG (2006) Principles of equal-channel angular pressing as a processing tool for grain refinement. *Prog Mater Sci* 51:881–981. doi:[10.1016/j.pmatsci.2006.02.003](https://doi.org/10.1016/j.pmatsci.2006.02.003)
- [10] Shih MH, Yu CY, Kao PW, Chang CP (2001) Microstructure and flow stress of copper deformed to large plastic strains. *Scripta Mater* 45:793–799. doi:[10.1016/S1359-6462\(01\)01098-3](https://doi.org/10.1016/S1359-6462(01)01098-3)
- [11] Suś-Ryszkowska M, Wejrzanowski T, Pakieła Z, Kurzydłowski KJ (2004) Microstructure of ECAP severely

- deformed iron and its mechanical properties. *Mater Sci Eng A* 369:151–156. doi:[10.1016/j.msea.2003.10.318](https://doi.org/10.1016/j.msea.2003.10.318)
- [12] Valiev RZ, Alexandrov IV, Zhu YT, Lowe TC (2002) Paradox of strength and ductility in metals processed by severe plastic deformation. *J Mater Res* 17:5–8. doi:[10.1557/JMR.2002.0002](https://doi.org/10.1557/JMR.2002.0002)
- [13] Dutkiewicz J, Masdeu F, Malczewski P, Kuku A (2009) Microstructure and properties of $\alpha + \beta$ brass after ECAP processing. *Arch Mater Sci Eng* 39:80–83
- [14] Neishi K, Horita Z, Langdon TG (2001) Achieving super plasticity in a Cu-40%Zn alloy through severe plastic deformation. *Scripta Mater* 45:965–970. doi:[10.1016/S1359-6462\(01\)01119-8](https://doi.org/10.1016/S1359-6462(01)01119-8)
- [15] Neishi K, Uchida T, Yamauchi A, Nakamura K, Horita Z, Langdon TG (2001) Low-temperature super plasticity in a Cu–Zn–Sn alloy processed by severe plastic deformation. *Mater Sci Eng A* 307:23–28. doi:[10.1016/S0921-5093\(00\)01970-5](https://doi.org/10.1016/S0921-5093(00)01970-5)
- [16] Kim HS, Kim WY, Song KH (2012) Effect of post-heat-treatment in ECAP processed Cu-40%Zn brass. *Alloys Compd* 536:200–203. doi:[10.1016/j.jallcom.2011.11.079](https://doi.org/10.1016/j.jallcom.2011.11.079)
- [17] Iwahashi Y, Wang J, Horita Z, Nemoto M, Langdon TG (1996) Principle of equal-channel angular pressing for the processing of ultra-fine grained materials. *Scripta Mater* 35:143–146. doi:[10.1016/1359-6462\(96\)00107-8](https://doi.org/10.1016/1359-6462(96)00107-8)
- [18] ASTM, E8 – 01 (2001) Standard test method for tension testing of metallic materials, No. T68
- [19] Jiang Y, Zhu R, Wang JT, You ZS (2016) An investigation on rolling texture transition in copper preprocessed by equal channel angular pressing. *J Mater Sci* 51:5609–5624. doi:[10.1007/s10853-016-9862-2](https://doi.org/10.1007/s10853-016-9862-2)
- [20] Su CW, Lu L, Lai MO (2006) A model for the grain refinement mechanism in equal channel angular pressing of Mg alloy from microstructural studies. *Mater Sci Eng A* 434:227–236. doi:[10.1016/j.msea.2006.06.103](https://doi.org/10.1016/j.msea.2006.06.103)
- [21] Sakai T, Belyakov A, Kaibyshev R, Miura H, Jonas J (2014) Dynamic and post-dynamic recrystallization under hot, cold and severe plastic deformation conditions. *Prog Mater Sci* 60:130–207. doi:[10.1016/j.pmatsci.2013.09.002](https://doi.org/10.1016/j.pmatsci.2013.09.002)
- [22] Padmavardhani D, Prasad YVRK (1991) Characterization of hot deformation behavior of brasses using processing maps: part II. β brass and α - β brass. *Metall Trans A* 22:2993–3001. doi:[10.1007/BF02650259](https://doi.org/10.1007/BF02650259)
- [23] Farabi E, Zarei-Hanzaki A, Pishbin MH, Moallemi M (2015) Rationalization of duplex brass hot deformation behavior: the role of microstructural component. *Mater Sci Eng A* 641:360–368. doi:[10.1016/j.msea.2015.06.042](https://doi.org/10.1016/j.msea.2015.06.042)